Supporting Information

A confinement strategy to prepare N-doped reduced graphene oxide foams with desired monolithic structures for supercapacitors

Daoqing Liu,[a,b,#] Qianwei Li, *[c,#] Si Li, [a,b] Jinbao Hou,[d] Huazhang Zhao *[a,b]

[a] Department of Environmental Engineering, Peking University, Beijing 100871, China

[b] The Key Laboratory of Water and Sediment Sciences, Ministry of Education, Beijing 100871, China

[c] State Key Laboratory of Heavy Oil Processing, Beijing Key Laboratory of Oil and Gas Pollution Control, China University of Petroleum, 18 Fuxue Road, Changping District, Beijing 102249, China

[d] College of Chemical Engineering, Beijing University of Chemical Technology, Beijing 100029, China

[#] Co-first author.

* Corresponding author.

Tel/fax: +86-10-62758748; email address: zhaohuazhang@pku.edu.cn (H.Z. Zhao).

Experimental Methods

1. Preparation of graphite oxide (GO)

Graphite oxide was prepared from natural graphite (Jinglong Co., Beijing, China) according to a modified Hummers method [1]: 120 mL 98 wt% H_2SO_4 was poured into a beaker containing a mixture of 5 g natural graphite and 2.5 g $NaNO_3$, and then the mixture was stirred in an ice bath for 30 min. 15 g $KMnO_4$ was added slowly into the mixture, which was allowed to react for 2 h at a temperature no more than 20°C. Then, the temperature was risen to 35°C, and the reaction was performed for another 2 h. After that, the reactant mixture was poured slowly into 360 mL distilled water under violent stirring condition so as to control the temperature no more than 90°C, followed by further reaction at 75°C for 1 h. After the mixture was diluted to 1.5 L, 50 mL 30 wt% H_2O_2 was added to consume the remaining $KMnO_4$ and the produced MnO_2. The as-obtained mixture was a bright yellow suspension. After filtered and washed with 5 wt% HCl and distilled water, the filter cake was freeze-dried for 24 h to obtain the graphite oxide.

2. Gas chromatography-mass spectroscopy (GC-MS) analysis

GC-MS analysis of the hydrothermal decomposition products of MF was carried out using a QP2010 ultra（Shimadzu，Kyoto, Japan) with an TR-WAXMS (Thermo Scientific， 30m×0.25mm×0.25μm) column. For GC-MS detection, Helium (99.999%) gas was used as carrier gas at a constant flow rate of 1 mL min^{-1}, and the injector temperature was maintained at 240°C. The oven temperature was programmed at 40°C (isothermal for 5 min), with an increase of 10°C min^{-1} to 240°C and maintained at this temperature for 20 min. The ion-source temperature was 200°C, mass spectra were taken with a fragment from 45to 500 Da.

Supplementary Figures and Tables

SEM Images of MF

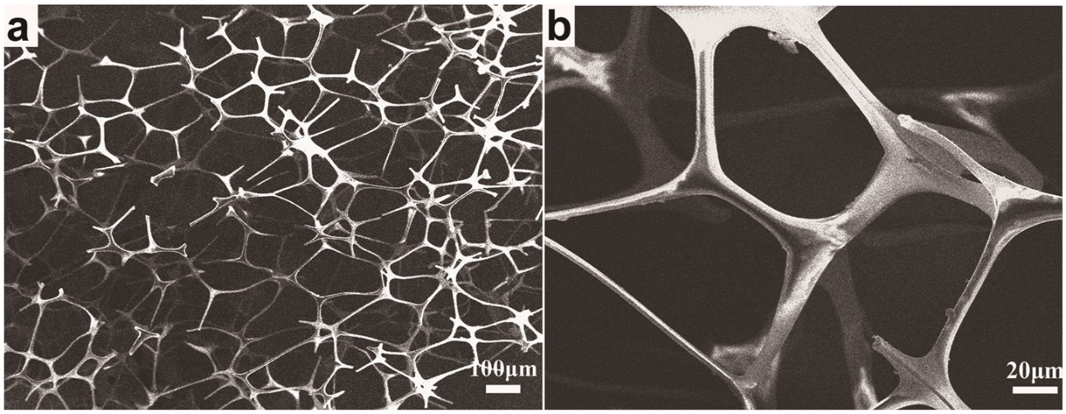

Figure S1. SEM images of MF at low (a) and high (b) magnifications.

Solubility of MF under different conditions

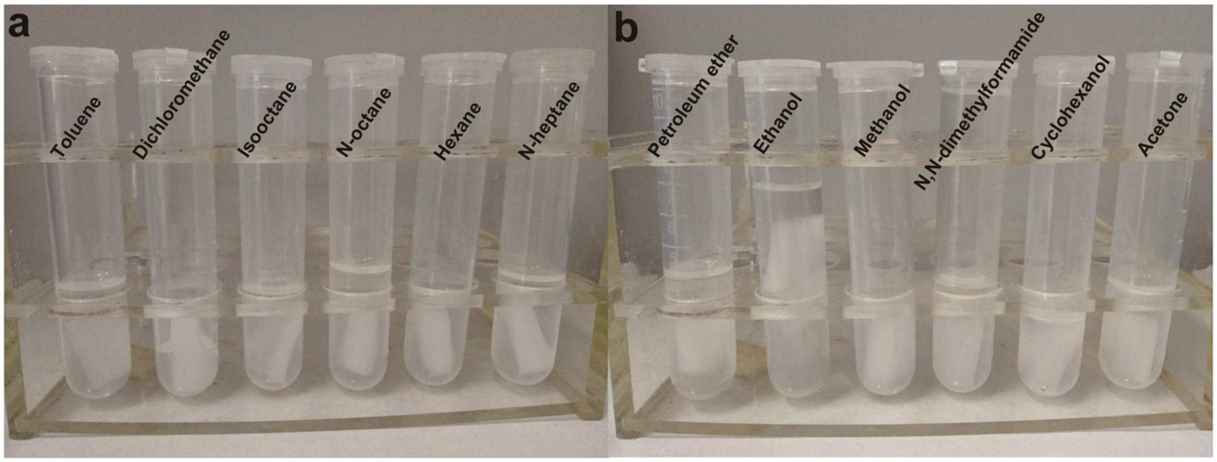

Figure S2. Solubility of MF sponge in different organic solvents.

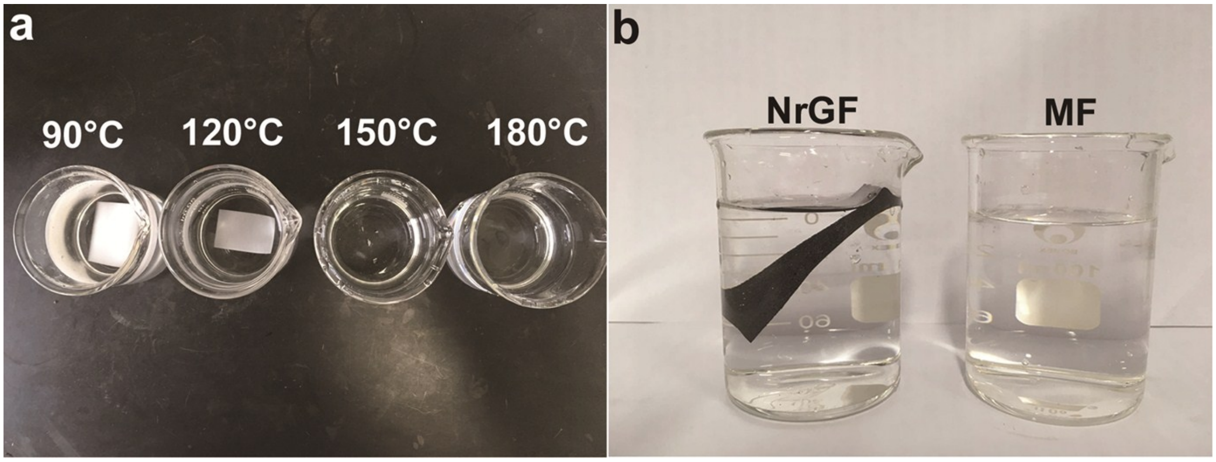

Figure S3. (a) The state of MF sponge after 6 h hydrothermal treatment at different temperatures. (b) Decomposition of MF-GO (left) and pure MF (right) after hydrothermal treatment at 180 °C for 6h in 10 wt% NH_4HCO_3 solution.

GC-MS results of hydrothermal decomposition products of MF

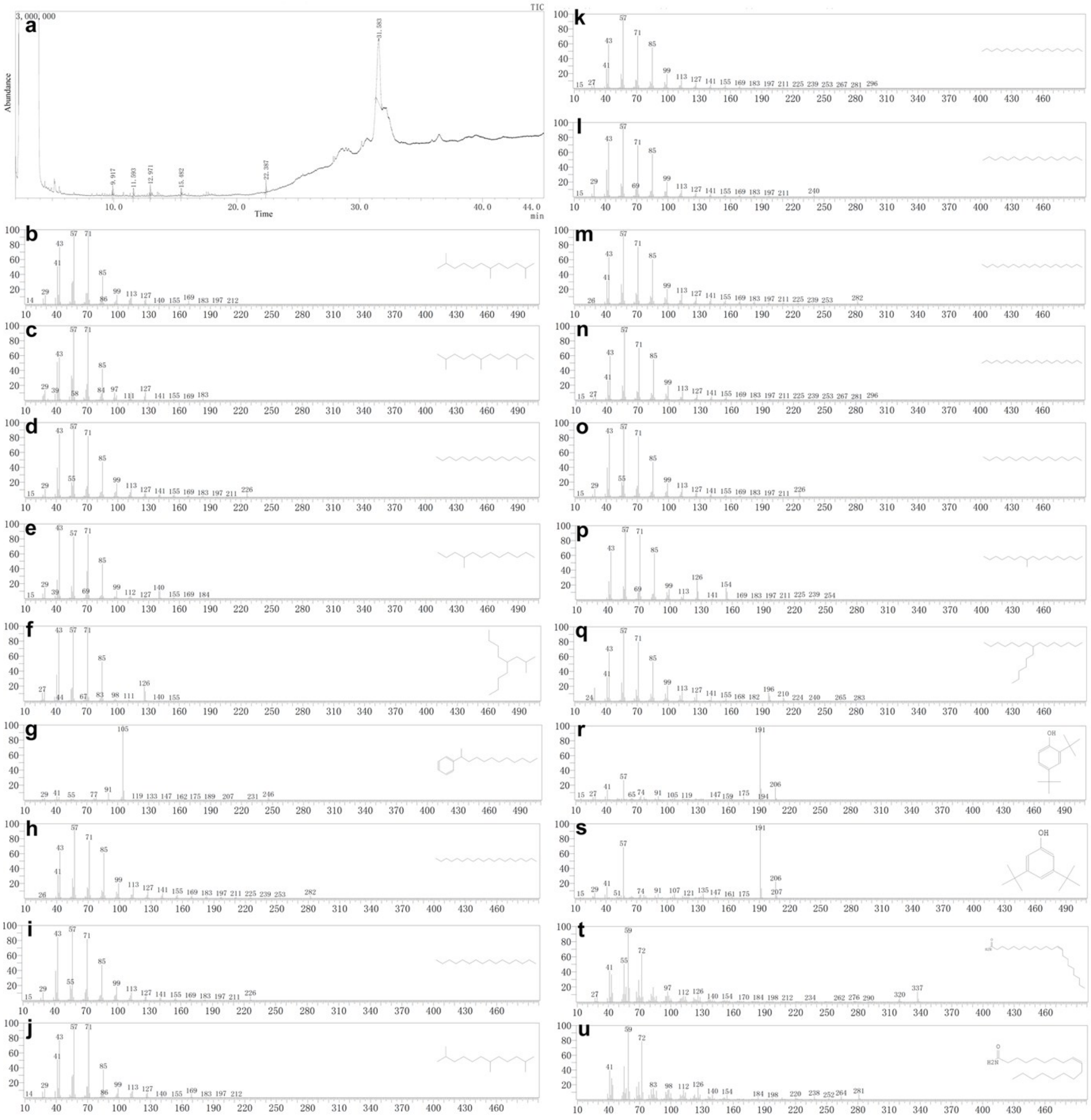

Figure S4. (a) GC-MS profile of hydrothermal decomposition products of MF. (b-u) Possible molecular structures of compounds present in hydrothermal decomposition products of MF using GC-MS analysis.

Table S1. Main organic matters detected by GC-MS in hydrothermal decomposition products of MF

Serial No.	Phytochemical compound	Formula	Molecular weight
1	Dodecane, 2,6,11-trimethyl-, 2,6,11-Trimethyldodecane	$C_{15}H_{32}$	212
2	Dodecane, 2,6,10-trimethyl-, Farnesane, 2,6,10-Trimethyldodecane	$C_{15}H_{32}$	212
3	Hexadecane, n-Cetane	$C_{16}H_{34}$	226
4	Dodecane, 4-methyl-, 4-Methyldodecane	$C_{13}H_{28}$	184
5	Nonane, 5-(2-methylpropyl)-, 5-Isobutylnonane	$C_{13}H_{28}$	184
6	Benzene, (1-methylundecyl)-, Dodecane, 2-Phenyldodecane	$C_{18}H_{30}$	246
7	Eicosane, n-Eicosane	$C_{20}H_{42}$	282
	n-Hexadecane, Cetane	$C_{16}H_{34}$	226
8	Dodecane, 2,6,11-trimethyl-, 2,6,11-Trimethyldodecane	$C_{15}H_{32}$	212
9	Heneicosane, n-Heneicosane, Henicosane	$C_{21}H_{44}$	296
10	Heptadecane, n-Heptadecane, Normal-heptadecane	$C_{17}H_{36}$	240
	Icosane, n-Icosane	$C_{20}H_{42}$	282
11	Eicosane, n-Eicosane, Icosane, n-Icosane	$C_{21}H_{44}$	296
12	Hexadecane, n-Cetane, n-Hexadecane, Cetane	$C_{16}H_{34}$	226
13	8-methyl-, 8-Methylheptadecane	$C_{18}H_{38}$	254
14	Pentadecane, 8-hexyl-, 8-n-Hexylpentadecane, 8-Hexylpentadecane	$C_{21}H_{44}$	296
15	Phenol, 2,4-bis(1,1-dimethylethyl)-, Phenol, 2,4-di-tert-butyl-	$C_{14}H_{22}O$	206
16	3,5-bis(1,1-dimethylethyl)-, 3,5-di-tert-butyl-, 3,5-Di-tert-butylphenol	$C_{14}H_{22}O$	206
17	13-Docosenamide, (Z)-, Erucylamide, Erucyl amide, (Z)-	$C_{22}H_{43}NO$	337
18	9-Octadecenamide, (Z)-, Oleic acid amide, Oleyl amide, Slip-eze	$C_{18}H_{35}NO$	281

SEM Images of GO/MF Composite

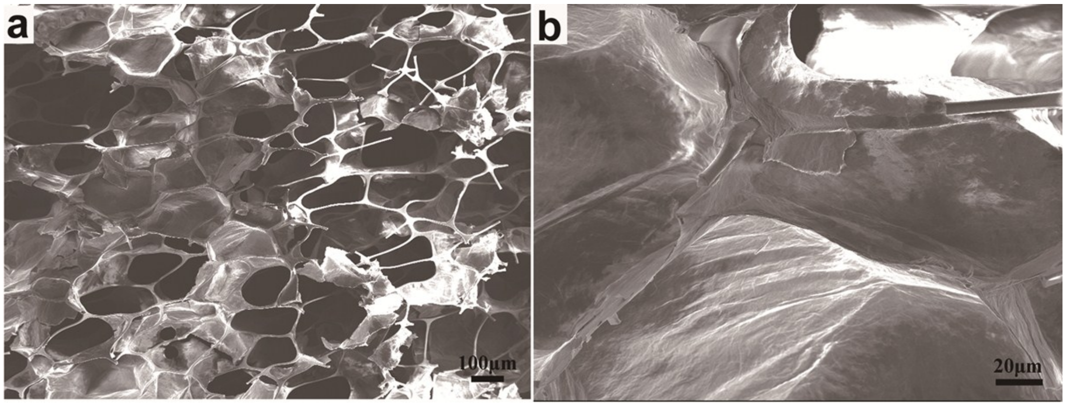

Figure S5. SEM images of GO/MF composite at low (a) and high (b) magnifications.

SEM Images of NrGF

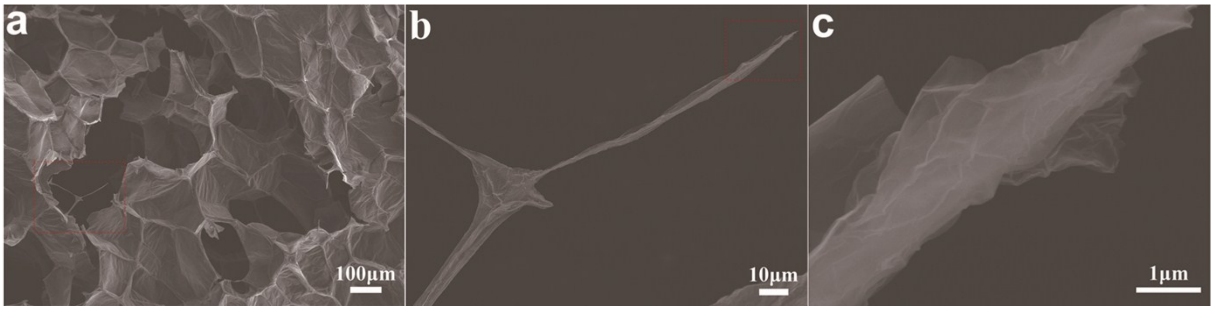

Figure S6. The SEM images of the rGO sheets coated on MF skeleton after the hydrothermal reduction process. (a) Low magnification image of NrGF sponge. (b) rGO sheets coated on the MF skeleton. (c) High magnification image of rGO sheets coated on MF skeleton.

SEM and Photo Images of rGF obtained in deioned water

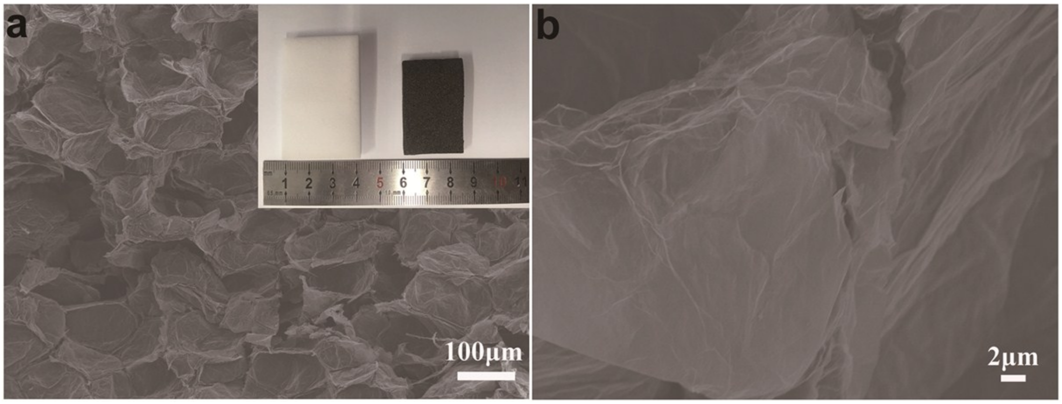

Figure S7. SEM images of reduced graphene foam (rGF) fabricated with deioned water in low (a) and high (b) magnifications.

Surface chemical state of NrGF obtained from EDS

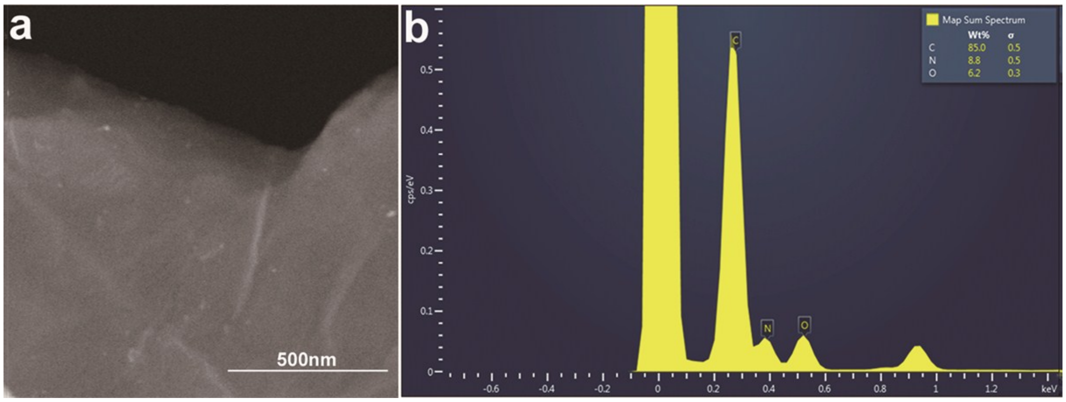

Figure S8. The energy dispersive spectrometer elemental (EDS) of NrGF by TEM.

Surface chemical state of rGF obtained from XPS

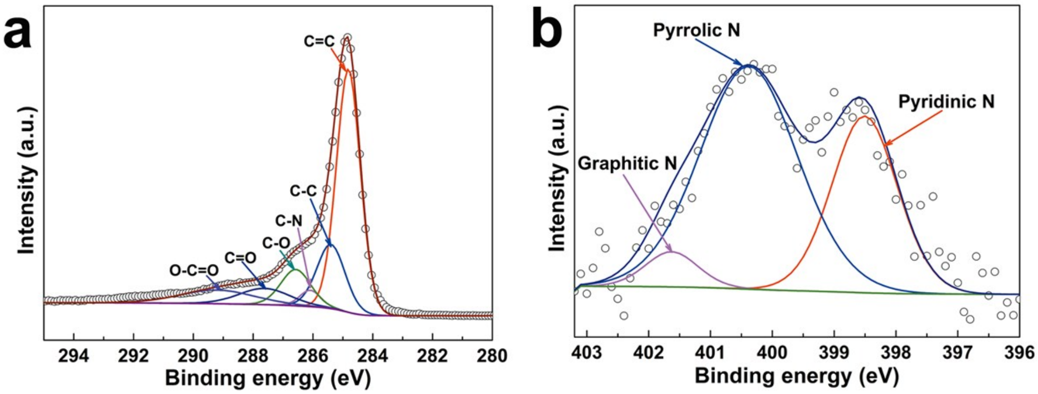

Figure S9. XPS spectra of the C1s region (a) and N 1s region (b) of the rGF.

Table S2. Surface elemental concentrations and relative contents of functional groups derived from C1s XPS spectra of GO , rGF and NrGF

Samples	C1s fitting binding energy (eV; relative percentage,%)					
	C=C(sp^2)	C-C(sp^3)	C-N	C-O	C=O	O-C=O
GO	284.8 (43.32)	285.4 (7.52)	-	287.0 (40.52)	287.5 (5.20)	288.8 (3.44)
rGF	284.8 (53.32)	285.4 (16.66)	286.09 (3.14)	286.9 (9.96)	287.53 (7.59)	289.0 (9.34)
NrGF	284.8 (55.26)	285.4 (17.81)	286.1 (10.76)	287.0 (4.46)	287.5 (4.67)	288.9 (7.03)

The electrochemical performance of rGF

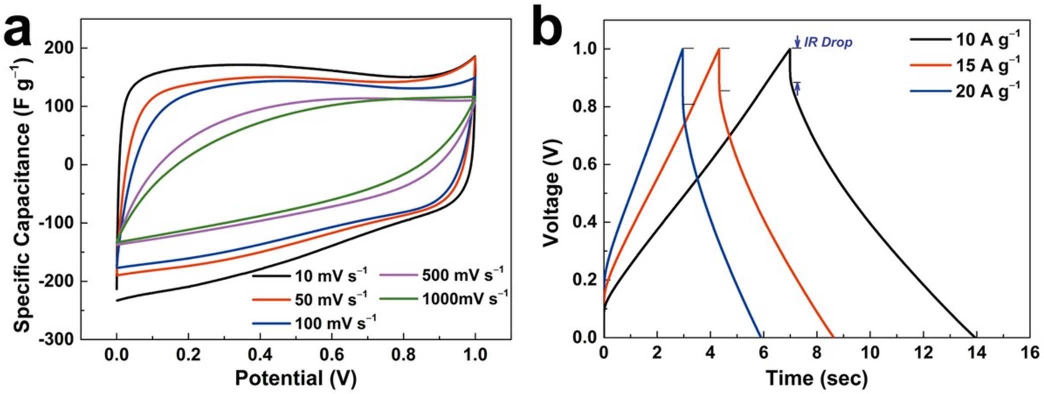

Figure S10. (a) CV curves of the rGF obtained at different scan rates. (b) Gravimetric charge/discharge curves of the rGF at different current densities.

Supplementary References

1. D. Liu, Q. Li and H. Zhao, *J. Mater. Chem. A*, 2018, **6**, 11471-11478.